Optical RF tone in-band labeling for large-scale and low-latency optical packet switches

Optical RF Tone In-Band Labeling for Large-Scale and Low-Latency Optical Packet Switches

Jun Luo, *Member, IEEE*, Harm J. S. Dorren, *Member, IEEE*, and Nicola Calabretta, *Member, IEEE*

***Abstract*—We propose an RF tone in-band labeling technique that is able to support large-scale and low-latency optical packet switch. This approach is based on N in-band wavelengths, each carrying M radio frequency (RF) tones. The wavelengths and the tones have a binary value, and are able to encode $2^{\mathrm{N}\times\mathrm{M}}$ possible routing address. We develop an optical label processor for the RF tone in-band optical label based on parallel and asynchronous processing. It allows the optical packet switch with an exponential increase of number of ports at the expense of limited increase in the latency and the complexity. By using RF tone in-band labeling technique, we demonstrate error free (bit error rate $<10^{-9}$) optical packet switching operation for both 160 Gb/s packets and 40 Gb/s packets. We further investigate the scalability, the latency and the optical power fluctuation tolerance of the proposed RF tone in-band labeling technique. We show that 30 label bits are able to be delivered using single in-band wavelength, and the label processor introduces an extra latency of less than 7 ns.**

***Index Terms*—Label processor, optical labeling, optical packet switching, RF tone in-band label.**

I. Introduction

As the overall performance of High Performance Computers (HPCs) and Data Centers (DCs) increases, high volumes of packetized data have to be transported among the clusters of thousands of servers within such machines. It requires switches that are capable to interconnect a large amount of nodes (large port count), allow for operation at high datarates, enable low end-to-end latency (for computing communications often end-to-end latency <1 μs is required [1]), and consume low energy. Whereas electronic switches that are used in current DCs have fundamental limits on the speed and the scalability of multi-rack electronic switching fabrics, and the associated power consumption by opto-electronic conversions, optical packet switches (OPS) which are featured of large scale and low latency may have potential to play a role in data center interconnects.

Manuscript received February 24, 2012; revised June 04, 2012; accepted June 04, 2012. Date of publication June 08, 2012; date of current version July 25, 2012. This work was supported in part by Chinese Scholarship Council under Grant [2010]3006 and by the Netherlands Science Foundation (NWO) and Netherlands Technology Foundation (STW) through the NRC Photonics and Vi programs.

J. Luo is with the COBRA Research Institute, Eindhoven University of Technology, 5600MB Eindhoven, The Netherlands, on leave from the School of Electronic Information Engineering, Tianjin University, 300072 Tianjin, China (e-mail: j.luo@tue.nl).

H. J. S. Dorren and N. Calabretta are with the COBRA Research Institute, Eindhoven University of Technology, 5600MB Eindhoven, The Netherlands (e-mail: n.calabretta@tue.nl; hdorren@tue.nl).

Color versions of one or more of the figures in this paper are available online at http://ieeexplore.ieee.org.

Digital Object Identifier 10.1109/JLT.2012.2204038

In OPS, optical labeling is usually employed to deliver the routing information that determines the forwarding of the optical packets. It is therefore that the number of the label bits which the optical labeling technique can carry, the complexity and the speed of the label processing will determine the scale and the latency of the OPS. For the optical labeling technique, one typical scheme is time multiplexing optical header, in which the label information is serial coded ahead of the packets in the time domain on the same wavelength [2], [3]. Guard times are needed between the label and payload so as to avoid any damages to the payload during the label erasure and insertion. Besides, this serial time multiplexing scheme consumes extra time to process the label, and requires sophisticated processing like serial to parallel conversion and synchronization at the label bit level. It thus introduces large latency and limits its scalability.

To address these issues, optical labeling techniques based on parallel multiplexing have been proposed and demonstrated during the years, such as optical code division multiplexing (OCDM) [4], [5], orthogonal multiplexing [6]–[8], subcarrier multiplexing (SCM) [9]–[13], and wavelength division multiplexing (WDM) [14], [15]. Whereas the parallel multiplexing offers the advantage of parallel processing of the label and payload, and thus the reduction of the latency, these labeling techniques may still have limits on the performance. The OCDM labeling will significantly increase the bit rate of the labels, and it is not easy to realize both the label generation and extraction. Orthogonal multiplexing exploits orthogonal modulation formats of the label and the payload [6]–[8]. But it needs to modulate the label on a nonzero payload signal which makes the payload suffer a low extinction ratio [7]. The SCM label is coded on a high subcarrier frequency with the label and the payload of the same wavelength [9]–[13]. However, the subcarrier frequency would place a limit to the bit rate of the payload in order to avoid possible spectrum overlapping between the payload and the label. Besides, the performance of the SCM label uses high subcarrier frequency, and may suffer from the fading effect due to the fiber dispersion. It is further limited by complicated and expensive electronics required in the label processing. WDM labeling exploits a separate wavelength to transmit the label [14], [15]. In this case, the optical label is transparent to the payload bit-rate and format. However, the WDM labeling may suffer from the fiber dispersion that causes the walk-off between the labels and payload, and it also consumes extra wavelength spectra resources. One thing should be noted that among these optical labeling schemes, the label bits are encoded in serial in time domain. It therefore consumes extra time just to synchronize and read all the label bits before processing the labels and producing the controlling signal to forward the payload. For example in [13], about 200 ns is required for the recognition of all the serial coded label bits, which is not acceptable for the high speed packets with short length (typically 75 ns packet length for 160 Gb/s packets).

To further reduce the latency of the OPS, parallel coding of the label bits together with in-band wavelength optical labeling are proposed [16]–[19]. In [16], we have employed parallel coded multiple in-band label wavelengths for the labeling of an OPS subsystem that is scalable to 4096 of ports. Essential in this approach is that 2^{N} addresses could be encoded by N parallel binary coded label wavelengths that are attached within the bandwidth of the payload [16], [17]. This approach allows the OPS to operate asynchronously at the expense of low power consumption and little latency. However, the number of the in-band label wavelengths that can be inserted could be ultimately limited by the amount of spectral bandwidth available. In order to further scale the OPS to address a larger number of ports, it is essential to increase the number of bits delivered by each in-band wavelength.

In this work, we propose to use the RF tone in-band labeling technique that is able to support large scale and low latency OPS. In this approach, each of the N in-band label wavelengths carries M binary coded radio frequency (RF) tones. In this way, the switch can address $2^{N\times M}$ possible ports (compared to 2^{N} for the case of only binary coded wavelength labeling [16]). We present the optical label processor (OLP) scheme for the RF tone in-band label, which allows for processing each label wavelength and RF tone in parallel at the expense of little latency. By using the RF tone in-band labeling, we experimentally demonstrated error free OPS operation for packets at data rate of 160 Gb/s and 40 Gb/s. Moreover, we discuss the scalability, the latency and the power fluctuation tolerance of the RF tone in-band labeling technique. We show that this labeling technique is able to deliver 30 label bits in one label wavelength, and introduce an extra latency of less than 7 ns.

This paper is organized as follows. Section II describes the concept of the RF tone in-band label technique and the optical label processor for the RF tone in-band label. In Section III, optical packet switching operation is demonstrated for 160 Gb/s as well as 40 Gb/s packets. Furthermore, the characteristic of the RF tone in-band labeling technique such as the scalability, the latency and the optical power fluctuation tolerance are discussed in Section IV. Finally, Section V summarizes the paper.

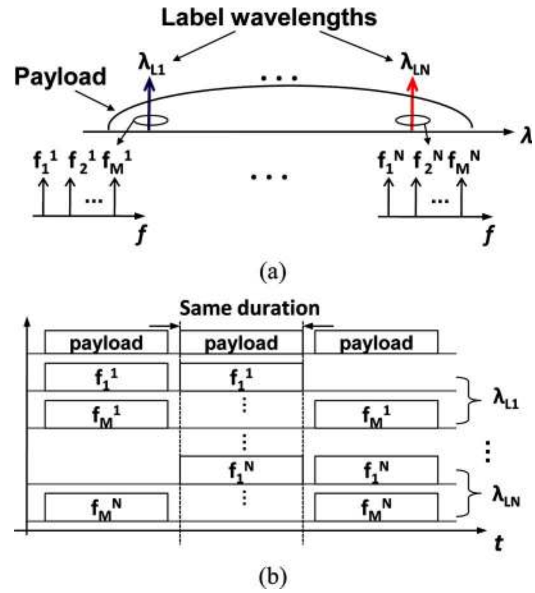

Fig. 1. The concept of the RF tone in-band label technique: (a) in the spectral domain and (b) time domain.

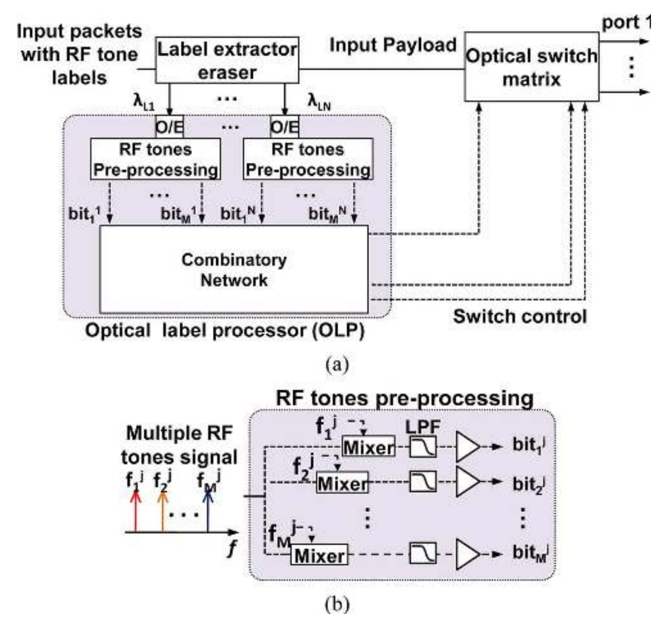

Fig. 2. (a) Schematic of the optical packet switch subsystem based on RF tone in-band labeling. (b) Implementation of the pre-processing block for the RF tone in-band optical label.

II. Concept of RF Tones In-Band Labeling

The concept of the RF tone in-band labeling technique is reported in Fig. 1. As is shown in Fig. 1(a), in this technique, N label wavelengths ($\lambda_{Lj}, j \in [1, N]$) are inserted within the payload spectrum bandwidth, and each label wavelength carries M RF tones (f_1^j to f_M^j). Each of the RF tones is binary coded, and represents one bit of the label (f_i^j represents $bit_i^j, i \in [1, M], j \in [1, N]$). Therefore, N in-band wavelengths with M RF tones are able to provide $N \times M$ label bits. This is M times larger than the in-band wavelength labeling technique [16]. Therefore, this labeling technique allows to address an exponential increase of the amount of ports in the OPS. Moreover, as is illustrated in Fig. 1(b), all the label bits have the same duration as the payload length. Thus, it allows to handle packets with variable lengths in an asynchronous fashion.

Fig. 2(a) illustrates the schematic diagram of the OLP for the RF tone in-band label. At the input of the OPS node, a label extractor/eraser is firstly used to extract the in-band label wavelengths from the input packets. The label extractor/eraser is built up by using a series of the passive narrow bandpass optical filters (e.g., a series of cascading FBGs or integrated comb filters). Especially in [20], we have presented an optical label extractor/eraser based on integrated mircoring resonator, which helps the integration of the switch node. The extracted label wavelengths are then processed by the OLP that determines the

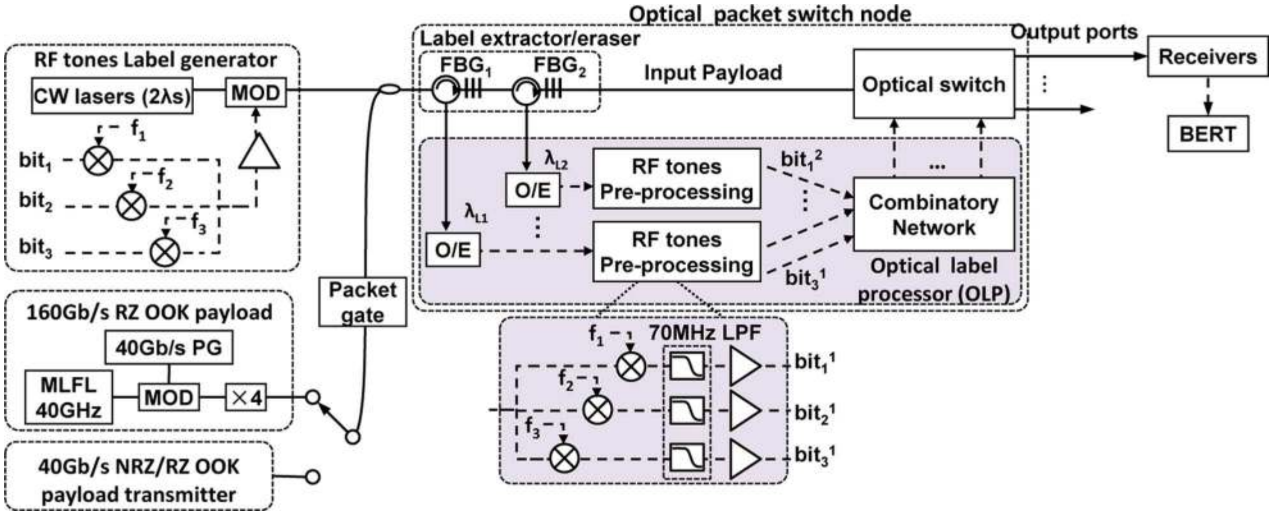

Fig. 3. Experimental setup of the optical packet switching subsystem for multiple data rate packets, MOD: optical modulator, MLFL: mode-locked fiber laser, PG: pattern generator, FBG: fiber Bragg grating, O/E: optical to electrical converter, LPF: low pass electrical filter, BERT: bit error rate tester.

packet destination by setting the optical switch. In the OLP, the label wavelengths are separately detected by the optical to electrical converter (O/E), and processed in parallel in the RF tones pre-processing blocks. The RF tones pre-processing blocks are used to extract the baseband label bit from the multiple RF tones signal. The obtained baseband label bits are finally combined together into the electrical combinatory network to generate the switching control signal, which decides the forwarding of the payload in the optical switch matrix.

Fig. 2(b) reports the detailed implementation of the RF tones pre-processing block. The multiple RF tones signal, which is obtained after the detection of the in-band label wavelength, is firstly divided into parallel paths and then experienced down-conversion by separately mixing with the frequencies at $\mathrm{f_i^j}$ $(\mathrm{i} \in [1, \mathrm{M}], \mathrm{j} \in [1, \mathrm{N}])$. After the mixing, the baseband label bits are selected out by the low-pass filter (LPF). Finally, the baseband label bits will be sent to the subsequent electrical combinatory network for the switching control generation. It is worth noting that the RF tones pre-processing blocks process all the RF tones labels asynchronously and in parallel. As a result, the OLP processing time can be kept constant regardless of the number of label wavelengths and RF tones. Moreover, all the electronic processing in the OLP can be implemented by a field programmable gate array (FPGA) board or in an application-specific integrated circuit (ASIC) for faster processing. It is therefore that this technique enables the OPS with an exponential increase of number of ports at the expense of limited increase in the latency and the complexity.

In the next section, we experimentally demonstrated OPS operation for multiple data rate packets of 160 Gb/s and 40 Gb/s by using the RF tone in-band labeling technique.

III. Demonstration of Optical Packet Switching for Multiple Data-Rate Packets

Fig. 3 shows the experimental setup of the optical packet switching for multiple data rate packets using RF tone in-band label technique. At the transmitter, two types of data payload are generated. Firstly, we generated the 160 Gb/s optical time division multiplexing (OTDM) return-to-zero (RZ) on-off keying (OOK) payload by time-quadrupling a 40 Gb/s data streams consisting of modulated $2^{11} - 1$ PRBS return-to-zero bits ($\lambda_{\mathrm{p1}} = 1546$ nm) using a fiber-based inter-leaver. The optical pulses have duration of 1.5 ps giving the −20 dB bandwidth of the 160 Gb/s payload to be 5 nm. Alternatively, 40 Gb/s NRZ and RZ OOK data stream ($\lambda_{\mathrm{p2}} = 1546.54$ nm) are directly generated by a 40 Gb/s optical transmitter (SHF 46210 C). A packet gate was used to generate data packet frames with 180 ns payload length separated with 25.8 ns of guard time. In the demonstration, we setup the OPS subsystem using two RF tone in-band label wavelengths. In the RF tone label generator, two in-band label wavelengths at $\lambda_{\mathrm{L1}} = 1544.3$ nm and $\lambda_{\mathrm{L2}} = 1546.8$ nm are generated with each label wavelength carrying three RF tones: $\mathrm{f_1^j} = 420$ MHz, $\mathrm{f_2^j} = 510$ MHz, and $\mathrm{f_3^j} = 615$ MHz (j = 1 or 2) to deliver 6 (2 × 3) label bits. As is shown in "RF tones Label generator" of Fig. 3, each baseband label bit is up converted by mixing with correspondingly one RF tone through a mixer (e.g., bit1 is mixing with RF tone f1). Binary coded RF tones are thus produced with each of them represents one label bit. Therefore, maximum 64 ports $(2^{2\times3})$ are able to be addressed by using only two label wavelengths.

Firstly, we investigate the OPS operation with 160 Gb/s OTDM payload. As is shown in Fig. 4(a), two RF tone in-band label wavelengths λ_{L1} and λ_{L2} are inserted within the −20 dB bandwidth of the 160 Gb/s OTDM payload. The optical powers of the label and payload are −3.9 dBm and 3.3 dBm, respectively. At the OPS node, the 160 Gb/s packets with RF tone in-band label is first passing through a label extractor/eraser consisting of two cascaded FBGs before being fed into the optical switch based on $\mathrm{LiNbO_3}$ technology [18]. The FBGs that are used for the extraction of the RF tone in-band labels have a Gaussian profile with 98% of reflectivity and 3 dB bandwidth of 6 GHz to avoid significant distortion to the payload due to the spectrum slicing. Fig. 4(b) and (c) show the electrical spectra of the multiple RF tones signals after the opto-electrical

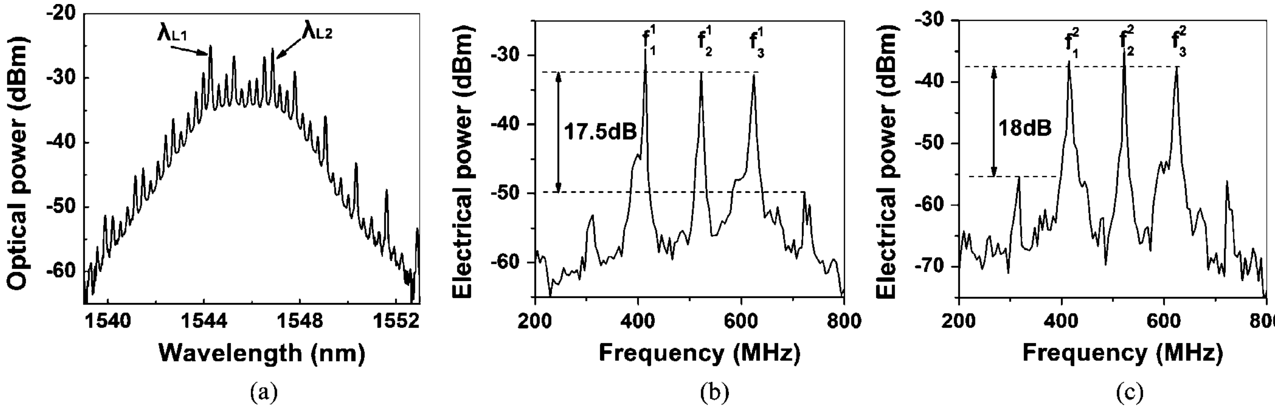

Fig. 4. (a) Optical spectra of the 160 Gb/s OTDM packets; the electrical spectra of the RF in-band label (b) λ_{L1} and (c) λ_{L2}.

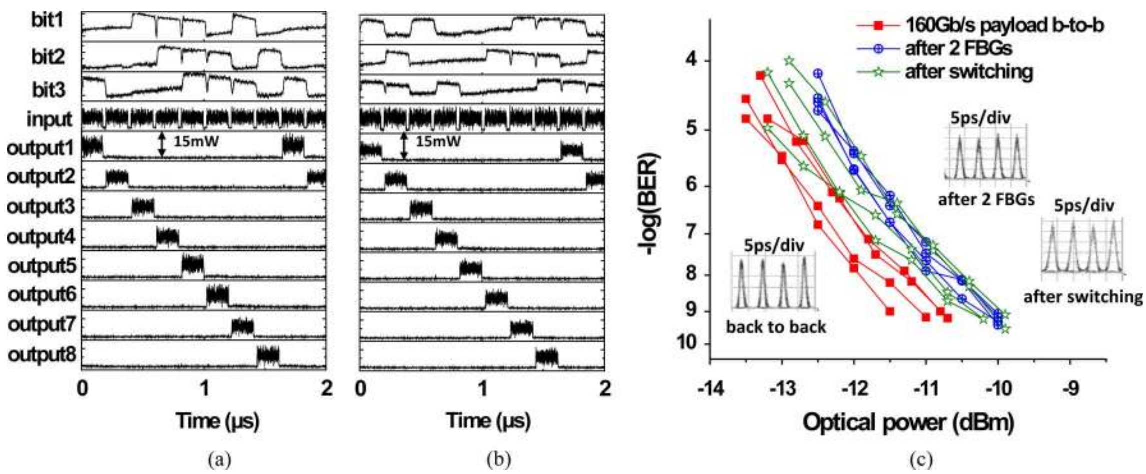

Fig. 5. Time traces of the 160 Gb/s OTDM packet switching results when using label bits obtained from (a) λ_{L1} and (b) λ_{L2}; (c) the BER curves of 160 Gb/s OTDM packets.

conversion of λ_{L1} and λ_{L2}, respectively. The power ratio between the RF tones and back ground noise peak is 17.5 dB and 18 dB for λ_{L1} and λ_{L2}, which indicates a high electrical signal to noise ratio of the electrical RF tone labels. Since at that time we have available only electrical combinatory networks with 3 input and 8 outputs, the 3 label bits for λ_{L1} and λ_{L2} were fed into two separate electrical combinatory networks. The outputs of the electronic combinatory networks control two separate 1×8 optical switches. Fig. 5(a) and (b) show the corresponding time traces of the switching results. The three graphs at the top shows the time traces of the extracted 3 label bits from λ_{L1} and λ_{L2}, respectively. The label bits have an eye-opening within the range of 0.4 to 0.65. Here, we define the eye-opening of a binary coded signal as [21]

$$\text{Eye}-\text{opening} = \frac{(\text{L1} - \sigma 1) - (\text{L0} + \sigma 0)}{(\text{L1} - \text{L0})}. \quad (1)$$

where L1, L0 is the mean of signal level 1 and level 0, and $\sigma 1, \sigma 0$ is the standard deviation of level 1 and level 0, respectively. The AC coupling behavior is observed in the time traces. It is due to the fact that the frequency mixers (Mini-Circuits ZX05-42 MH+) with a lower cut-off frequency of the intermediate frequency (IF) of 5 MHz were used in the RF tone label generation and processing. A better eye-opening could be obtained if the IF of the mixer starts from DC. The time traces of the switched payload are also reported in Fig. 5(a) and (b). Fig. 5(c) shows the BER curves of the 160 Gb/s OTDM packets at three different positions in the system. The four curves of each group correspond to the four 40 Gb/s tributaries of the 160 Gb/s OTDM signal. First, the back-to-back BER curves (red solid square) are reported as reference. The green stars represent the BER measured after the label extractor. Finally, the blue circle cross show the BER measured at the output port 1 of the 1×8 broadcast and select switching. Note that we reported only the BER result of one output port since the BER curves measured at the other broadcast and elect switch outputs are very similar. Error free operation is achieved, and the extraction of two cascading FBGs and the switching operation caused 0.5 dB and 0.7 dB penalty respectively. Eye diagrams of the 160 Gb/s packets can be found in the insets of Fig. 5(c). Clear eye diagrams also show that distortion to the signal quality is negligible during the switching operations.

Furthermore, we also carried out optical packet switching operation for 40 Gb/s non-return to zero (NRZ) and RZ OOK packets, which have much narrower spectrum bandwidth. For the 40 Gb/s NRZ and RZ OOK packets, the label wavelength was at $\lambda_{L2} = 1546.8$ nm which is displaced of 0.26 nm with respect to the central wavelength of payload. The optical powers

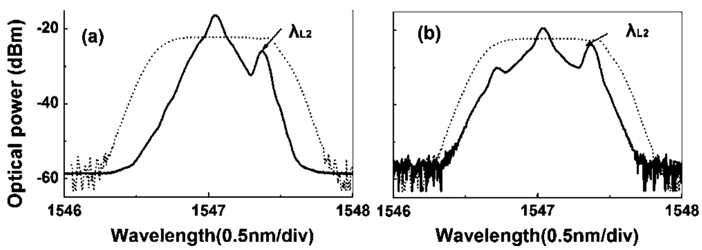

Fig. 6. Optical spectra of (a) 40 Gb/s NRZ packets and (b) 40 Gb/s RZ packets.

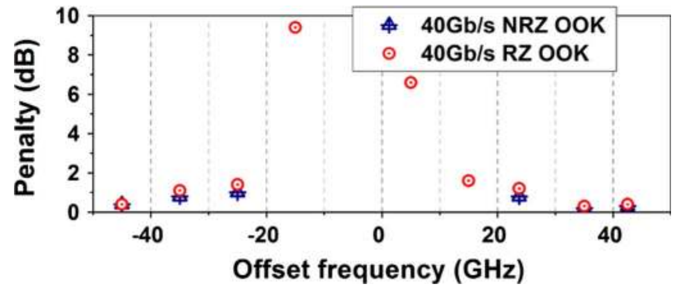

Fig. 7. Penalty to the 40 Gb/s packets caused by the label extraction with the label placed at offset frequency to payload center.

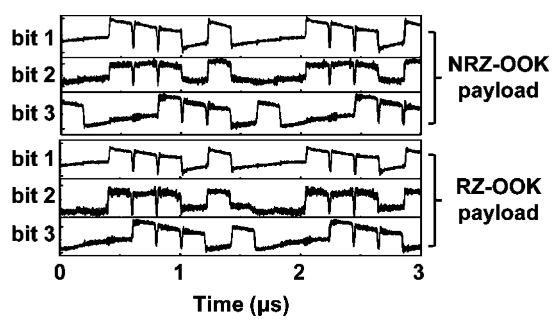

Fig. 8. Time traces of the extracted label bits of 40 Gb/s NRZ packets (top) and 40 Gb/s RZ packets (bottom).

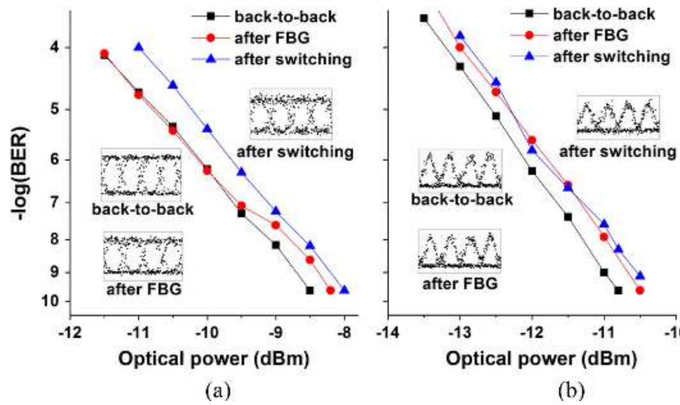

Fig. 9. BER curves of (a) 40 Gb/s NRZ packets and (b) 40 Gb/s RZ packets.

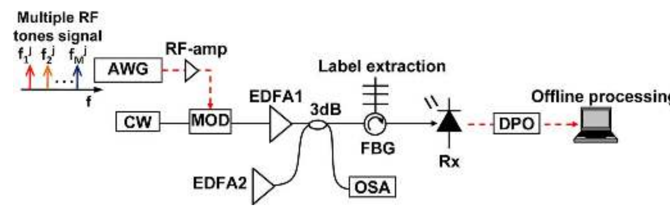

Fig. 10. Experimental setup of the investigation on the RF tone in-band label. AWG: arbitrary waveform generator; RF-amp: RF wideband amplifier; CW: continuous wave laser source; MOD: optical modulator; EDFA: erbium doped fiber amplifier; FBG: fiber Bragg grating; OSA: optical spectrum analyzer; Rx: optical receiver; DPO: digital phosphor oscilloscope.

of the label and payload are −6.8 dBm and 3.2 dBm, respectively. Fig. 6(a) and (b) show the optical spectra of NRZ packets and RZ packets, respectively. The dotted traces in Fig. 6(a) and (b) show the filter profile of a 100 GHz optical WDM channel centered at λ_{p2}, which indicates that the optical label is located within the 100 GHz WDM channel bandwidth. Fig. 7 shows the measured penalties of the payload due to the spectrum carving by the label extractor at different wavelength offset with respect to the payload central wavelength. When the label is located beyond 30 GHz far away to the payload central wavelength, the penalties due to the spectrum carving are less than 1 dB. It indicates that this in-band labeling technique has the potential to be employed even for the data packets with narrow spectrum bandwidth (<40 GHz). Fig. 8 shows the time traces of the extracted label bits from the RF tone label. The eye openings of the obtained label bits are no less than 0.4 both in the case of using NRZ payload and RZ payload. BER measurements of the 40 Gb/s payload are carried out both after the label extraction and the switching. Fig. 9 shows that error free operation of the OPS with penalty of 0.5 dB and 0.4 dB was obtained for 40 Gb/s NRZ and 40 Gb/s RZ OOK packets, respectively. Open eye diagrams before and after switching of the 40 Gb/s NRZ and RZ packets can also be found in the insets of Fig. 9. One should note that only 0.3 and 0.2 dB penalty respectively was measured for 40 Gb/s NRZ and RZ OOK packets after the carving of one FBG.

IV. Discussions on RF Tone In-Band Labeling

In order to support large scale and low latency OPS, the optical labeling technique is expected to be able to address large number of ports $(>2^{10})$ and introduce little latency during the label processing $(\sim\text{ns})$. It is therefore that we further investigate the scalability, the latency and the tolerance of the optical power fluctuation of the RF tone in-band labeling based on the experimental setup in Section III. For the simplicity of the discussion, we only assess the performance of generation, extraction and processing of one RF tone in-band label wavelength here, and thus use a simplified experimental setup. Note that In [17], we have shown that the cascading 6 FBGs to extract up to 6 in-band label only caused less than 0.7 dB penalty, which is a slightly increase with respect to the label extraction operation with a single FBG. It is therefore expected that the results obtained by using the simplified setup (shown in Fig. 10) still provide a good estimation of the scalability of the proposed labeling technique. As shown in Fig. 10, the electrical multiple RF tone label is produced by an arbitrary waveform generator (AWG, Tektronix AWG 7122B), and amplified by a 10 Gb/s wideband RF amplifier (RF-amp) before driving the optical modulator to generate the optical RF tone label. The optical label is boosted by EDFA1 and then combined with an ASE source produced by

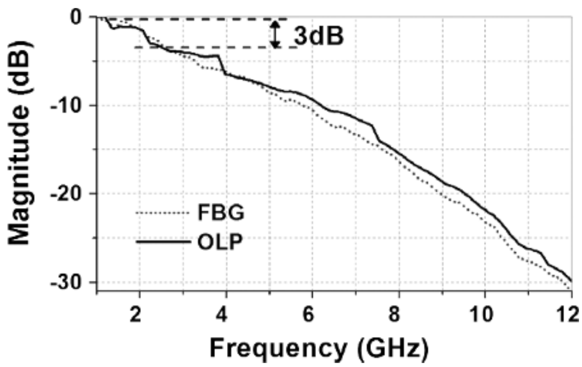

Fig. 11. The measured frequency response of the OLP (solid) and FBG (dotted).

EDFA2 in order to adjust the OSNR of the optical label. The label extractor/eraser consists of the same FBG that is used in the demonstration in Section III. After extraction, the optical label is detected by a 10 Gb/s optical receiver (Rx, Aglient lightwave converter 11982A). The Rx responses linearly with the input power range from -15 dBm to -3 dBm and starts to introduce significant nonlinear distortion with input power >4 dBm. The detected RF label is then sampled by a real time digital phosphor oscilloscope (DPO, Tektronix DPO 72004). The data samples acquired in the DPO are offline processed. Here, Matlab programming is used to simulate the RF tone label processing as is described in Section II and evaluate the signal quality of the extracted label bits from the RF tone label. During the investigation, the sampling rate of both the AWG and the DPO is 6.25 GSamples/s. The RF tone label has a symbol rate of 10 MSymbol/s, and a duration of 80 ns with 20 ns guard times.

A. Scalability

The amount of ports of the OPS that can be controlled is determined by the amount of label bits carried by the optical label. As each RF tone is representing one label bit, it is therefore important to investigate how many RF tones can be carried by one in-band wavelength. In this section, we discuss the maximum number of RF tones that can be allocated in one label wavelength based on the setup in Fig. 10.

Firstly, we measured the frequency response of the OLP by using a lightwave component analyzer (HP 8703). The 3-dB bandwidth of the OLP is around 2.5 GHz for one label wavelength as shown by the solid trace in Fig. 11. As a comparison, Fig. 11 also shows the frequency response of the FBG (dotted trace). It is visible that the bandwidth of the OLP is mainly limited by narrow bandwidth of the FBG used in the label extraction. Although using a larger bandwidth FBG can improve the available bandwidth, it may also introduce higher penalty due to the spectrum carving of the payload.

Secondly, we look for the proper frequency spacing between the RF tones to allocate as many as possible tones within the limited bandwidth of one label wavelength. It is known that denser is the frequency spacing between RF tones, larger amount of tones can be carried by the in-band wavelength. However, the crosstalk between the RF tones will increase with smaller frequency spacing, and hence require higher order filter to separate them in the OLP. Here, we carry out the investigation using RF

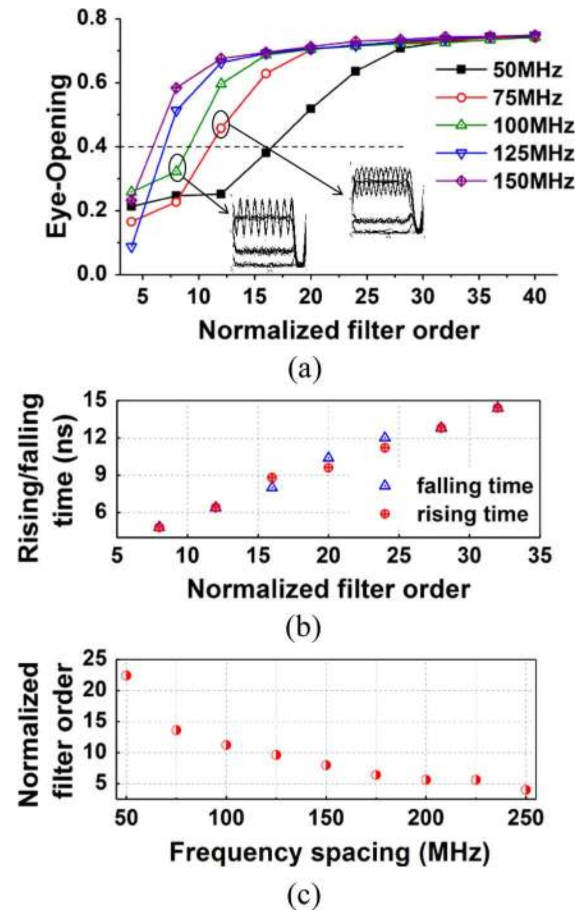

Fig. 12. (a) The eye-opening of the obtained label bits when using RF tones of different frequency spacing and filter order in the OLP; (b) the rising/falling time of the label bits versus the filter order; (c) the minimum required filter order to obtain label bits with eye opening larger than 0.4.

tone label carrying 3 RF tones with different frequency spacing. We evaluate the eye opening of the label bits after the label processing with different filter order in the OLP. As in the digital filter design, the filter order varies linearly with the sampling rate for the same filter profile. To simplify the discussion, we define the normalized filter order as

$$\text{Normalized filter order} = \frac{\text{filter order (a.u.)}}{\text{Sampling rate (in GSamples/s)}}. \quad (2)$$

Fig. 12(a) and (b) show the results when varying the frequency spacing of the RF tones and filter order. The figures show that although improved eye-opening of the label bits is given by employing higher order filter, this will cause longer filter delay and slower output rising/falling time. As a result, both the latency and the guard times of the OPS will increase. Besides, Fig. 12(a) also indicates that the eye-opening is not improving further when the normalized filter order is over a certain threshold, e.g., the threshold filter order is around 15 at the frequency spacing of 100 MHz. Besides, as is indicated by the eye diagrams shown in Fig. 12(a), it can be found that the eye-opening to sufficiently recognize the label bits should be larger than 0.4. Thus, taking an eye-opening of 0.4, Fig. 12(c) shows the minimum required normalized filter order

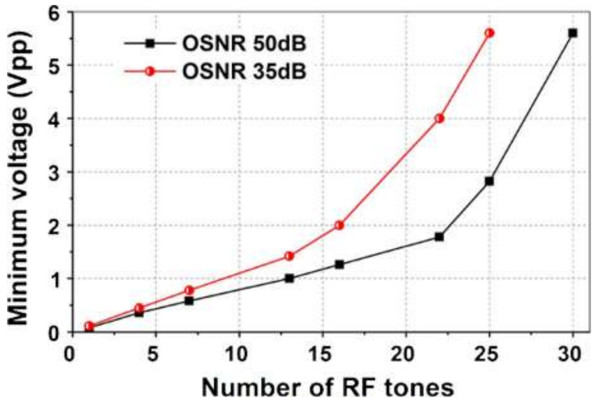

Fig. 13. Minimum required voltage to drive the modulator to guarantee the obtained label bits with eye opening larger than 0.4.

for different frequency spacing of the RF tones. According to Fig. 12(b) and (c), with frequency spacing larger than 100 MHz, normalized filter order around 10 is already sufficient to detect label bits with eye-opening of 0.4 and rising/falling time of less than 6 ns. Therefore, considering RF tones with 100 MHz spacing and normalized filter order of 10, potentially more than 25 RF tones in a single wavelength can be allocated within the 3-dB bandwidth of the OLP.

Another important parameter to be considered in defining the maximum number of tones is the linearity of the optical modulator. A minimum voltage V_{pp} of each RF tone to drive the modulator should be guaranteed so that the detected label bit of each tone has an eye-opening of at least 0.4. When scaling the number of RF tones to M, it will result in a total peak to peak voltage of $M \times V_{pp}$. To avoid any distortion during the modulation, the maximum allowed voltage to drive the optical modulator is $V\pi$ ($V\pi = 6$ V for the $LiNbO_3$ modulator used in the setup in Fig. 10). Therefore, the number of RF tones that can be allocated in one label wavelength will be further limited by $V\pi$. Fig. 13 shows the minimum required V_{pp} of the multiple RF tones label to drive the modulator in order to achieve eye-opening larger than 0.4. We take the measurements with the frequency spacing of 100 MHz while increasing the number of RF tones. Investigates are carried out at the optical signal to noise ratio (OSNR) of both 50 dB and 35 dB. At the OSNR of 50 dB, at least 80 mV_{pp} is required for delivering a single RF tone, while 5.6 V_{pp} are required for delivering 30 tones. At the OSNR of 35 dB, a larger voltage of 112 mV_{pp} is required to deliver a single RF tone, and only 25 tones can be delivered by using 5.6 V_{pp} (this is close to $V\pi$ of the modulator) to drive the modulator. Thus, the maximum number of RF tones that can be delivered using one label wavelength is around 30.

According the above discussions, we experimentally investigate the delivering of 30 RF tones in a single wavelength by using the setup shown in Fig. 10. In the experiment, the OSNR was 50 dB, the modulator drive voltage was 5.6 V_{pp}, and the frequency spacing of the RF tones is 100 MHz. All the 30 label bits are coded by different $2^{15} - 1$ PRBS data to have different combinations. Fig. 14 shows the time traces of the received RF tone label (top) and the recovered 30 label bits from the 30 RF tones after the label processing respectively. Fig. 15(a) shows that the eye-openings of all the 30 label bits are larger than 0.4. The insets in Fig. 15(a) also show the eye diagrams of the label bits at 100 MHz, 2.4 GHz and 3 GHz. Fig. 15(b) shows the electrical spectra of the 30 received RF tones. It can found that the peak power of each the RF tone directly determines the eye-openings that can be achieved. As compared to the frequency response shown in Fig. 11, it can be concluded that the variations of the peak power and the eye opening of the RF tones are mainly due to frequency response of the system. A better performance might be achieved if pre-emphasis of the system frequency response is implemented during the optical label generation.

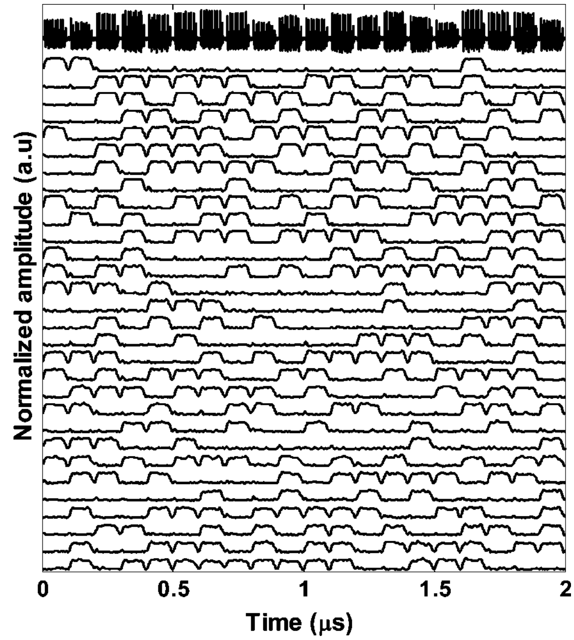

Fig. 14. Time traces of the received RF tone label (top) and extracted 30 label bits (the rest).

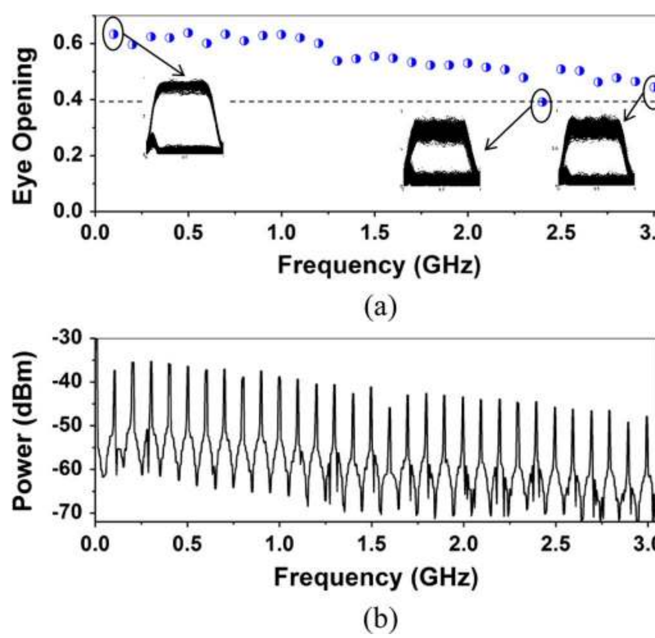

Fig. 15. (a) Eye opening of the extracted 30 label bits (insets show the corresponding eye diagrams). (b) Electrical spectra of the RF tone in-band label with 30 tones.

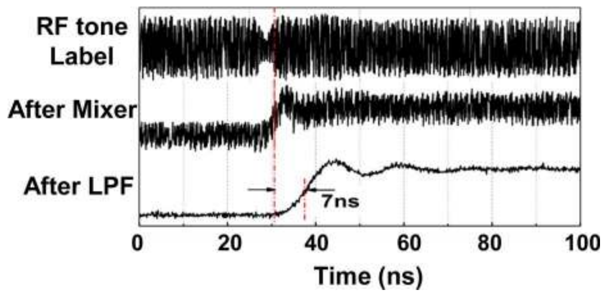

Fig. 16. The time delay introduced by the RF tone pre-processing block.

These results verified that based on the setup in Fig. 10, the RF tone labeling technique is able to deliver 30 RF tones by using only one label wavelength. If we consider more label wavelengths, the number of label bits can increase exponentially. (In [17] we have shown that the insertion/extraction of the 6 in-band label wavelength only introduces less than 0.7 dB penalties to the 160 Gb/s payload. The low penalty indicates that by using 6 in-band label wavelengths, each carrying 30 RF tones, the in-band RF tone labeling technique can potentially deliver 180 (30×6) label bits, and thus coding more than 2^180 optical addresses.

B. Latency of the Optical Label Processor

The latency of the optical label processor determines the time it required to setup the switch matrix for switching. The optical label processor proposed here for the RF tone label mainly consists of two parts: one is the pre-processing of the RF tones, which extracts the baseband label bits from the RF tones subcarrier; the other part is the routing controlling which processes the label bits and generates the corresponding switch control signal according the routing algorithm. Both the RF pre-processing and routing controlling will contribute to the total latency of the OLP. In [16], we reported that the combinatory network introduces 3 ns delay, and the parallel implementation of the combinatory network allows for processing large number of address bits with slightly increase in delay. In this subsection, we focus on the extra latency that is introduced by the pre-processing block. As is pointed out in Section II, with the parallel processing, the latency of the pre-processing block equals the delay of its one parallel path. Therefore, in Fig. 16, we show the measured delay in each part in one parallel path of the RF tone pre-processing block based on the setup in Fig. 3. The delay caused by the pre-processing is 7 ns, which is mainly contributed by the low pass filter (Mini-Circuits SLP-70). The delay time is expected to be further reduced by using low pass filter of optimized design [22]. Besides, as is discussed in Section II, with the OLP processing all the RF tones and label wavelength in a parallel and synchronous fashion, the OLP can process RF tone labels carrying large amount of label bits with little latency increase.

C. Power Fluctuation Tolerance of the Optical Label Processor

Practically, the optical power fluctuation of the labels might occur because of the distortion caused by the filtering, or by the switching, or along the transmission system. Therefore, it is important to investigate the power fluctuation tolerance of the OLP. For the OLP in the setup of Fig. 10, the power fluctuation tolerance can be assessed by look into the minimum required input optical power at the optical receiver in order to achieve the received label bits with an eye opening larger than 0.4. Fig. 17 shows the measured results while increasing the number of the RF tones. It is found that the tolerance to power fluctuation tolerance decreases as the number of RF tones increase. For instance, considering ~ 4 dBm as the maximum allowed input power to the optical receiver in order to avoid significant nonlinear distortion, the power fluctuation tolerance with input OSNR of 35 dB is 6 dB when delivering 13 RF tones, and further decreased to 0.5 dB for delivering 25 tones. With such a small tolerance range, 25 RF tones is the maximum number of tones can be delivered when $\mathrm{OSNR} = 35$ dB. While $\mathrm{OSNR} = 50$ dB, the power fluctuation tolerance is 11 dB for 13 RF tones and drops to 1 dB for 30 tones. Comparing the two curves at OSNR of 35 dB and 50 dB, it can be found that a larger power fluctuation is tolerated with a higher input OSNR. Besides, one thing should be noted that the tolerance to input power fluctuation also depends on the response linearity of the receiver used in the OLP. It is believed that if a highly linear photodiode is employed in the OLP a larger tolerance range of the power fluctuation can be obtained.

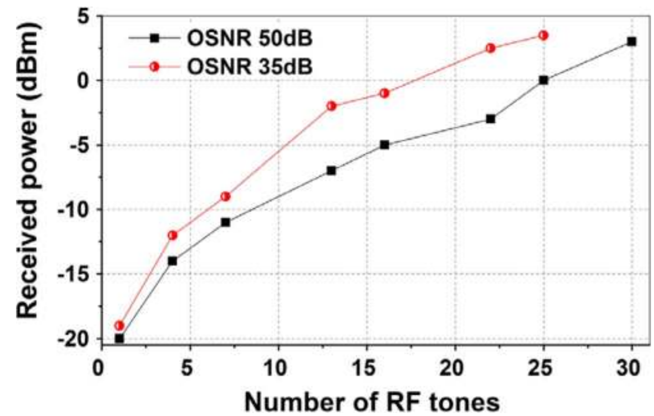

Fig. 17. Minimum required input optical power to the OLP versus the number of RF tones carried by one label wavelength.

V. Conclusion

We have proposed a novel in-band optical labeling technique based on N in-band label wavelengths, each of the wavelength carrying M binary coded RF tones to provide $N \times M$ label bits. The advantage of this technique is that the label processor can process all the label bits in parallel and asynchronously. This has allowed very fast processing time of 7 ns independently of the number of label bits. Based on the RF tone in-band optical labeling technique, we have experimentally demonstrated error free optical packet switching operations for both 160 Gb/s RZ OOK packets and 40 Gb/s NRZ/RZ-OOK packets, with the penalty of 0.7 dB, 0.5 dB and 0.4 dB respectively. The results in the latter case also indicates that this in-band labeling technique has the potential to be employed for the data packets with narrow spectrum bandwidth (<40 GHz). We investigated the performance of the optical RF tone in-band labeling including the scalability, the latency and the optical power fluctuation tolerance of OLP. We show that at least 30 label bits can be delivered in a single label wavelength, with around 7 ns extra latency. These results show that the presented optical RF tone in-band labeling technique has the potential to provide large number of label bits with fast processing time, and thus enables to control an optical switch with large amount of ports at the expense of low latency.

ACKNOWLEDGMENT

The authors would like to acknowledge Dr. F. Gomez-Agis, Y. Shi, and N. Sotiropoulos for helps on the 160 Gb/s setup and AWG operation.

REFERENCES

[1] R. Hemenway, R. Grzybowski, C. Minkenberg, and R. Luijten, "Optical-packet-switched interconnect for supercomputer applications [Invited]," *J. Opt. Networking*, vol. 3, pp. 900–913, 2004.
[2] C. Guillemot *et al.*, "Transparent optical packet switching: The European ACTS KEOPS project approach," *J. Lightw. Technol.*, vol. 16, no. 12, pp. 2117–2134, Dec. 1998.
[3] F. Ramos *et al.*, "IST-LASAGNE: Towards all-optical label swapping employing optical logic gates and optical flip-flops," *J. Lightw. Technol.*, vol. 23, no. 10, pp. 2993–3011, Oct. 2005.
[4] N. Wada, G. Cincotti, S. Yoshima, N. Kataoka, and K. Kitayama, "Characterization of a full encoder/decoder in the AWG configuration for code-based photonic Routers—Part II: Experiments and applications," *J. Lightw. Technol.*, vol. 24, no. 1, pp. 113–121, Jan. 2006.
[5] N. Wada, H. Furukawa, and T. Miyazaki, "Prototype 160-Gbit/s/port optical packet switch based on optical code label processing and related technologies," *IEEE J. Sel. Topics Quantum Electron.*, vol. 13, no. 5, pp. 1551–1559, Sep.—Oct. 2007.
[6] N. Chi *et al.*, "Transmission and optical label swapping for 4×40 Gb/s WDM signals deploying orthogonal ASK/DPSK labeling," *IEEE Photon. Technol. Lett.*, vol. 17, pp. 1325–1327, 2005.
[7] A. M. Koonen *et al.*, "Label-controlled optical packet routing—technologies and applications," *IEEE J. Sel. Topics Quantum Electron.*, vol. 13, no. 5, pp. 1540–1550, Sep.–Oct. 2007.
[8] A. M. Koonen *et al.*, "Optical packet routing using orthogonal labelling—Results from the FP5 STOLAS project," in *Proc. ECOC*, 2005, paper Mo.4.4.1.
[9] N. Chi, J. Zhang, and P. Jeppesen, "All-optical subcarrier labeling based on the carrier suppression of the payload," *IEEE Photon. Technol. Lett.*, vol. 15, no. 5, pp. 781–783, May 2003.
[10] L. Chung-Li, D. J. Sabido, P. Poggiolini, R. T. Hofmeister, and L. G. Kazovsky, "CORD—A WDMA optical network: Subcarrier-based signaling and control scheme," *IEEE Photon. Technol. Lett.*, vol. 7, no. 5, pp. 555–557, May 1995.
[11] A. K. Mishra *et al.*, "Spectrally compact optical subcarrier multiplexing with 42.6 Gbit/s AM-PSK payload and 2.5 Gbit/s NRZ labels," *Electron. Lett.*, vol. 42, pp. 1303–1304, 2006.
[12] X. Bo *et al.*, "First field trial of OLS network testbed with all-optical contention resolution of asynchronous, variable-length optical packets," in *Proc. OFC/NFOEC*, 2007, paper OMJ6.
[13] G. P. Leguizamon, B. Ortega, and J. Capmany, "Advanced subcarrier multiplexed label swapping in optical packet switching nodes for next generation internet networks," *J. Lightw. Technol.*, vol. 27, no. 6, pp. 655–669, Mar. 2009.
[14] I. M. White, M. S. Rogge, K. Shrikhande, and L. G. Kazovsky, "A summary of the HORNET project: A next-generation metropolitan area network," *IEEE J. Sel. Areas Commun.*, vol. 21, no. 9, pp. 1478–1494, Nov. 2003.
[15] N. Wada, H. Harai, W. Chujo, and F. Kubota, "80G to 10G bit/s variable rate photonic packet routing based on multi-wavelength label switch," in *Proc. ECOC*, 2001, paper We.B.2.3.
[16] W. Wang *et al.*, "Scalable optical packet switching at 160 Gb/s data rate," in *Proc. ECOC*, 2009, paper 4.6.3.
[17] N. Calabretta, H.-D. Jung, E. Tangdiongga, and H. J. S. Dorren, "All-optical packet switching and label rewriting for data packets beyond 160 Gb/s," *IEEE Photon. J.*, vol. 2, no. 2, pp. 113–129, Mar. 2010.
[18] N. Calabretta, W. Wang, T. Ditewig, O. Raz, F. G. Agis, S. Z. H. de Waardt, and H. J. S. Dorren, "Scalable optical packet switches for multiple data formats and data rates packets," *IEEE Photon. Technol. Lett.*, vol. 22, no. 7, pp. 483–485, Jul. 2010.
[19] N. Calabretta, F. Gomez-Agis, H. de Waardt, and H. J. S. Dorren, "First demonstration of OPS and burst detection of 160 Gb/s packets through three 52 km-spaced optical nodes," in *Proc. OFC*, 2011, paper OMK3.
[20] N. Calabretta *et al.*, "All-optical label extractor/eraser for in-band labels and 160-Gb/s payload based on microring resonators," *IEEE Photon. Technol. Lett.*, vol. 21, no. 9, pp. 560–562, May 2009.
[21] "Analyzing data using eye diagrams," Agilent, 2009. [Online]. Available: http://na.tm.agilent.com/plts/help/WebHelp/Analyzing/Analyzing_Data_using_Eye_Diagrams.html
[22] K. Nayebi, T. P. Barnwell, III, and M. J. T. Smith, "Low delay FIR filter banks: Design and evaluation," *IEEE Trans. Signal Process.*, vol. 42, no. 1, pp. 24–31, Jan. 1994.

Jun Luo (M'12) received the Ph.D. degree in optical communications from Tianjin University, Tianjin, China, in 2012.

From 2010 to 2011, he was a Visiting Researcher with the COBRA Research Institute, Eindhoven University of Technology, Eindhoven, The Netherlands, where he is currently a Postdoctoral Researcher. His current research interests include optical packet switching and high-speed optical signal processing.

Harm J. S. Dorren (M'12) received the M.Sc. degree in theoretical physics and Ph.D. degree from Utrecht University, Utrecht, The Netherlands, in 1991 and 1995, respectively.

He joined Eindhoven University of Technology, Eindhoven, The Netherlands, in 1996, where he presently serves as a Full Professor and Scientific Director of the COBRA Research Institute. Between 1996 and 1999, he was also a part-time research associate with KPN-Research in The Netherlands. In 2002, he was a Visiting Researcher with the National Institute of Industrial Science and Technology (AIST), Tsukuba, Japan. In 2002, he received a VIDI grant and in 2006 a VICI grant by The Netherlands Organization for Scientific Research. His research interests include optical packet switching, digital and ultrafast photonics, and optical interconnects. He has authored and coauthored over 380 journal papers and conference proceedings.

Prof. Dorren has served as an associate editor for the IEEE JOURNAL OF QUANTUM ELECTRONICS between 2005 and 2009. In 2010, he co-chaired an IEEE winter topical meeting on Optical Interconnects and he serves(d) as a member of the program committees for leading international conferences in his field such as ECOC, OFC, CLEO-Europe, Photonics and Switching and COIN. In 2012, he will act as one of the TPC chairs for the European Conference on Optical Communications and for the Conference on Photonics and Switching.

Nicola Calabretta (M'04) received the B.S. and M.S. degrees in telecommunications engineering from Politecnico di Torino, Turin, Italy, in 1995 and 1999, respectively, and the Ph.D. degree from the COBRA Research Institute, Eindhoven University of Technology, Eindhoven, The Netherlands, in 2004.

In 1995, he visited the RAI Research Center, Turin, Italy. From 2004 to 2007, he was a Researcher with Scuola Superiore Sant'Anna University, Pisa, Italy. He is currently with the COBRA Research Institute, Eindhoven University of Technology, Eindhoven, The Netherlands. He has coauthored more than 150 papers published in international journals and conferences and holds three patents. His fields of interest are optical packet switching, semiconductor optical amplifier, all-optical wavelength conversion and regeneration, and advanced modulation formats for optical packet switching.

Dr. Calabretta is currently acting as a reviewer for several IEEE, IEE, and OSA journals.